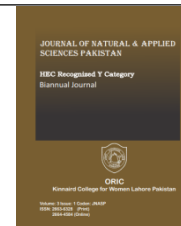




Contents list available <http://www.kinnaird.edu.pk/>

Journal of Natural and Applied Sciences Pakistan

Journal homepage: <http://jnasp.kinnaird.edu.pk/>



A MATHEMATICAL MODEL FOR PREDICTION OF TEMPERATURE AND CONCENTRATION PROFILES OF CHEMICAL SPECIES IN NONISOTHERMAL MULTIPLE-COMPARTMENT SYSTEMS

Oludare Adedire^{1*}, J.N. Ndam²

¹Department of Mathematics, University of Jos, Nigeria

²Federal College of Forestry Jos, Plateau State, Nigeria

Article Info

*Corresponding Author

Email: dharens@gmail.com

Abstract

A mathematical model for investigating the spatio-temporal patterns of temperature and concentration profiles of chemical species moving through a no isothermal multiple-compartment system is derived. The no isothermal system which consists of adjacent compartments whose partitions allow endothermic reaction is considered with the requirement that energy has to be supplied at an elevated temperature to trigger reaction rate of the reacting chemical species. Particularly, this research used process parameters for pyrolysis of propane commonly used in the production of ethylene which is an important industrial gas. The derived mathematical model – based on distributed parameter approach and unidirectional transport of chemical species– consists of a system of coupled Partial Differential Equations (PDEs) which are discretised spatially using the Method of Lines (MOL) technique and the resulting semi-discrete system in one independent variable t is solved using MATLAB ode15s solver which has been known to be well optimised for solutions of such problems. The results showed that as the reacting chemical species moved spatially through the interconnected no isothermal system, there is decrease in temperature profile as a result of significant conversion due to chemical process of the species being transported thereby causing decrease in temperature at some time t . However, temperature begins to rise due to constant wall temperature until a steady state is attained when significant conversion of reacting species in chemical reaction has been accomplished. Also, a reduction in concentration profile due to consumption in reaction of chemical species is observed as the spatial distance covered by the chemical species increases.

Keywords

Mathematical, Model, temperature, concentration, Non-isothermal, Multiple-Compartment.



1. Introduction

Reactions taking place in chemical reactors are largely dependent on the temperature and concentration profiles of the system. Adequate regulation of temperature and moderate addition of chemical substance could affect concentration of chemical species and contribute to optimum yield of products in such reactor system. Some past researches have involved chemical kinetics and were based on lumped parameter approach (Manion & Mcgivern, 2016; Kiss & Osz, 2017; Ball 1998). Nelson and Balakrishnan (2008) modelled lumped parameter system when considering auto ignition of hydrocarbons in a batch reactor. The chemical component of their model contained four chemical species undergoing six reactions. They indicated the possibility of having non physical solutions whenever the steady state temperature is greater than certain values. Watson (1908) investigated the rate of disinfection with change in concentration of disinfectant based on lumped parameter system and some of his results are based on findings of Chick (1908). The result obtained in the case of phenol in his study indicated a reaction of seventh order and concluded that such results may be said to be extraordinary because of rare existence of reaction order greater than third order. Readers may check the literature (Borisov *et al.*, 2012; Audenaert *et al.*, 2010) and references contained therein on some kinetic models based on lumped parameter systems. Lumped parameter systems involving kinetic models are those which usually lead to Ordinary Differential Equations (ODEs)

which could not capture spatiotemporal properties of chemical species in chemical reactors. In order to solve some of the problems associated with limitations of lumped parameter systems, alternate approach is to use distributed parameter system which often involve Partial Differential Equations (PDEs). Adedire and Ndam (2019) used distributed parameter system to investigate chlorine concentration in a multiple-compartment system. Their model was based on isothermal system and they concluded that the developed mathematical model could effectively predict chlorine concentration through bulk water and intermediate sections consisting of biofilms of *P. Aeruginosa* with humic acid. Sharma *et al.* (2015) also modelled transport phenomena using distributed parameter system. They used reduced model for square-shaped monolithic channel where elliptic PDEs were reduced to a set of parabolic PDEs and an ODE in the flow channel with 2-D elliptic PDEs in the wash coat layer. Further details on models based on distributed parameter system leading to PDEs can be found in the works of Orava *et al.* (2015) and Crapulli *et al.* (2010). Distributed parameter system has the advantage of leading to a system of PDEs which could show more detailed behaviour of any chemical species moving through the reactor. The major challenge is that the numerical solution of the system of PDEs is far more complex than numerical solutions of ODEs obtained from lumped parameter systems. However, with the availability of modern computers with adequate processing speed,

numerical computations of distributed parameter systems can be achieved with moderate accuracy of solutions. Motivation to proceed with this study is hinged on the observation that there has not been research findings on modelling temperature and concentration profiles for chemical species transport through non isothermal multiple-compartment systems which are connected at boundaries. Previous researches on interconnected multiple-compartment reactors (Adedire & Ndam, 2019; 2020a; 2020b) were based on isothermal systems. Consideration of non-isothermal system will aid the formulation of a mathematical model for the transport of chemical species whose reaction rate constant is not based on assumption of constant temperature through interconnected systems. This will also enable designers of chemical reactors gain insight into behaviour of chemical species whose reaction rate is dependent on temperature changes in multiple-compartment system. The aim of this study is to derive a mathematical model capable of predicting temperature and concentration profiles for species transport through non isothermal multiple-compartment reactor with interconnected boundaries. The specific objective of the study is to investigate transport of chemical species involving endothermic chemical reaction – based on process parameters for pyrolysis of propane in the production of ethylene through interconnected multiple-compartment reactor using distributed parameter system. The

remaining part of this paper is organized as follows: section 2 presents model development, section 3 deals with numerical simulation, while section 4 is on results and discussion and conclusion comes up in section 5.

2. Model Development

In this section, the governing model equations shall be developed based on assumption of treating fluid as a continuum (Thompson, 1972). Energy balance shall be coupled with mass balance to give the set of equations which shall be solved simultaneously in order to investigate the effects of temperature changes on concentration profile of chemical species being transported through the non isothermal interconnected multiple-compartment system.

Let $T_{\xi}(\bar{x}, t): \Omega \times \mathbb{R} \rightarrow \mathbb{R}$ and $\Psi_{\phi}(\bar{x}, t): \Omega \times \mathbb{R} \rightarrow \mathbb{R}$ be functions representing the temperature and concentration in a medium with boundary $\partial\Omega$ containing species ξ such that $\bar{x} \in \Omega^n$, $\bar{x} = x_1, x_2, \dots, x_n$, $n \in \mathbb{N}$ are spatial coordinates and t is time. Let $q \in \mathbb{N}$ be total number of compartments and $\gamma \in \{A, B, C, D, E\}$ be the set representing five compartments A, B, C, D and E respectively. With unidirectional flow assumption, $\bar{x} = x_1$ and let $x_1 = x$ represent x -axis, the schematic representation and procedure used by Adedire and Ndam (2020a) are shown in Figure 1.

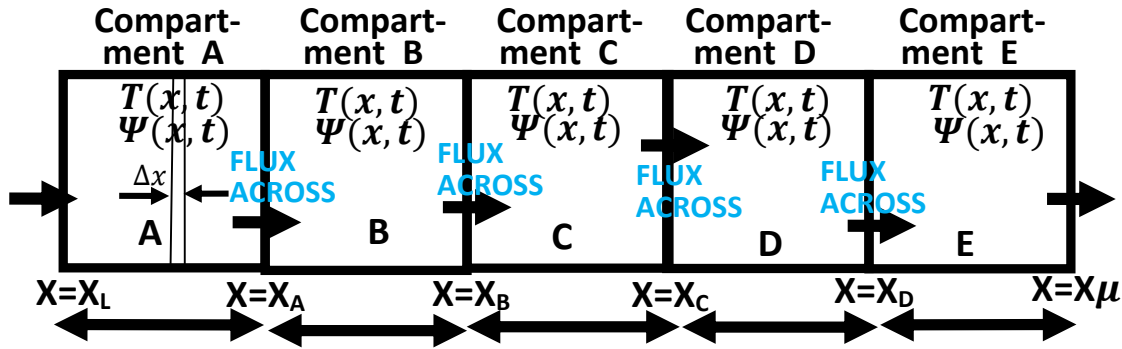


Figure 1: Species transport in interconnected multiple-compartment system.

For $q = 1; \gamma = A; n = 1; x_1 = x$, the energy balance and mass balance equations are set up with the assumption that heat flux and flow occur along the x-axis. The chemical species is assumed to diffuse non isothermally such that ξ undergoes irreversible homogeneous p^{th} order reaction kinetics for some $p \in \mathbb{N}$. Let $q_{h\gamma\xi}$ be heat flux

across the q -compartment system with assumption that the reaction rate constant $k_{\gamma\xi}$ and the temperature $T(x, t)_{\gamma\xi}$ have nonlinear relationship and follow Arrhenius equation (Connors, 1990), $\gamma \in \{A, B, C, D, E\}$. Thus, for $p=1$, energy balance over infinitesimal thickness in the x direction of γ^{th} compartment gives

$$\begin{aligned}
 (\Delta x)T(x, t)_{\gamma\xi} \Big|_t - (\Delta x)T(x, t)_{\gamma\xi} \Big|_{t+\Delta t} &= vT(x, t)_{\gamma\xi} \Big|_x \Delta t - vT(x, t)_{\gamma\xi} \Big|_{x+\Delta x} \Delta t \\
 &+ q_{h\gamma\xi} \Big|_x \Delta t - q_{h\gamma\xi} \Big|_{x+\Delta x} \Delta t + \frac{\Delta H k_{\gamma o} e^{-\left(\frac{E}{RT_{\gamma\xi}}\right)} \Psi(x, t)_{\gamma\xi}}{\rho C_f} \Delta x \Delta t \quad (1)
 \end{aligned}$$

Divide (1) through by $\Delta x \Delta t$ gives

$$\begin{aligned}
 \frac{T(x, t)_{\gamma\xi} \Big|_t - T(x, t)_{\gamma\xi} \Big|_{t+\Delta t}}{\Delta t} &= -v \frac{T(x, t)_{\gamma\xi} \Big|_x - T(x, t)_{\gamma\xi} \Big|_{x+\Delta x}}{\Delta x} \\
 &- \frac{q_{h\gamma\xi} \Big|_x \Delta t - q_{h\gamma\xi} \Big|_{x+\Delta x}}{\Delta x} + \frac{-\Delta H k_{\gamma o} e^{-\left(\frac{E}{RT_{\gamma\xi}}\right)} \Psi(x, t)_{\gamma\xi}}{\rho C_f} \quad (2)
 \end{aligned}$$

Taking the limit of (2) as $\Delta x \rightarrow 0, \Delta t \rightarrow 0$ gives

$$\begin{aligned}
 \frac{\partial T(x, t)_{\gamma\xi}}{\partial t} &= -v_\gamma \frac{\partial T(x, t)_{\gamma\xi}}{\partial x} - \frac{\partial q_{h\gamma}}{\partial x} + \frac{-\Delta H k_{\gamma o} e^{-\left(\frac{E}{RT_{\gamma\xi}}\right)} \Psi(x, t)_{\gamma\xi}}{\rho C_f} \quad (3)
 \end{aligned}$$

where ΔH heat of reaction is, C_f is fluid specific heat, v_γ is linear fluid velocity, $k_{\gamma o}$ is specific rate constant, E is activation energy, R is gas constant, and ρ is fluid density.

Analogously, mass balance over infinitesimal thickness Δx in x-direction of γ^{th} compartment of the reactor for $p=1$ with flux $q_{h\gamma\xi}$ for concentration $\Psi(x,t)_{\gamma\xi}$ of species ξ gives

$$(\Delta x) \Psi(x,t)_{\gamma\xi} \Big|_t - (\Delta x) \Psi(x,t)_{\gamma\xi} \Big|_{t+\Delta t} = v \Psi(x,t)_{\gamma\xi} \Big|_x \Delta t - v \Psi(x,t)_{\gamma\xi} \Big|_{x+\Delta x} \Delta t + q_{h\gamma\xi} \Big|_x \Delta t - q_{h\gamma\xi} \Big|_{x+\Delta x} \Delta t + \left[-k_{\gamma o} e^{-\left(\frac{E}{RT_{\gamma\xi}}\right)} \Psi(x,t)_{\gamma\xi} \Delta x \Delta t \right] \quad (4)$$

Division of (4) by $\Delta x \Delta t$ gives

$$\frac{\Psi(x,t)_{\gamma\xi} \Big|_t - \Psi(x,t)_{\gamma\xi} \Big|_{t+\Delta t}}{\Delta t} = -v_{\gamma x} \frac{\Psi(x,t)_{\gamma\xi} \Big|_x \Delta t - \Psi(x,t)_{\gamma\xi} \Big|_{x+\Delta x} \Delta t}{\Delta x} - \frac{q_{h\gamma\xi} \Big|_x \Delta t - q_{h\gamma\xi} \Big|_{x+\Delta x} \Delta t}{\Delta x} - k_{\gamma o} e^{-\left(\frac{E}{RT_{\gamma\xi}}\right)} \Psi(x,t)_{\gamma\xi} \quad (5)$$

Taking the limit of (5) as $\Delta x \rightarrow 0$, $\Delta t \rightarrow 0$ gives

$$\frac{\partial \Psi(x,t)_{\gamma\xi}}{\partial t} = -v \frac{\partial \Psi(x,t)_{\gamma\xi}}{\partial x} - \frac{\partial q_\xi}{\partial x} - k_{\gamma o} e^{-\left(\frac{E}{RT_\xi}\right)} \Psi(x,t)_{\gamma\xi} \quad (6)$$

Using Fourier law of heat flux with the assumption that thermal conductivity and axial fluid velocity are constant, equation (3) becomes

$$\frac{\partial T(x,t)_{\gamma\xi}}{\partial t} = -v_\gamma \frac{\partial T(x,t)_{\gamma\xi}}{\partial x} + \frac{k}{\rho C_f} \frac{\partial}{\partial x} \left(\frac{\partial T(x,t)_{\gamma\xi}}{\partial x} \right) - \frac{\Delta H k_{\gamma o} e^{-\left(\frac{E}{RT_{\gamma\xi}}\right)} \Psi(x,t)_{\gamma\xi}}{\rho C_f}, \quad x_L \leq x \leq x_\mu, t \geq 0 \quad (7)$$

Using Fick's law of diffusion (Tyrrell, 1964; Crank, 1979) then equation (6) becomes

$$\frac{\partial \Psi(x,t)_{\gamma\xi}}{\partial t} = -v \frac{\partial \Psi(x,t)_{\gamma\xi}}{\partial x} + \frac{\partial}{\partial x} \left(D \frac{\partial \Psi(x,t)_{\gamma\xi}}{\partial x} \right) - k_{\gamma o} e^{-\left(\frac{E}{RT_{\gamma\xi}}\right)} \Psi(x,t)_{\gamma\xi}, \quad x_L \leq x \leq x_\mu, t \geq 0 \quad (8)$$

and (8) with assumed constant diffusivity gives

$$\frac{\partial \Psi(x, t)_{\gamma\xi}}{\partial t} = -v \frac{\partial \Psi(x, t)_{\gamma\xi}}{\partial x} + D \frac{\partial^2 \Psi(x, t)_{\gamma\xi}}{\partial x^2} - k_{\gamma o} e^{-\left(\frac{E}{RT_{\gamma\xi}}\right)} \Psi(x, t)_{\gamma\xi}, x_L \leq x \leq x_{\mu}, t \geq 0 \quad (9)$$

Observe that equations (7) and (9) are coupled system of partial differential equations which will be solved simultaneously in each γ^{th} compartment of the multiple compartment system. Hence,

equations (7) and (9) for $q=5$ for $\gamma \in \{A, B, C, D, E\}$ depicted in Figure 1 give the following system of PDEs which are coupled in each compartment.

$$\frac{\partial T(x, t)_{A\xi}}{\partial t} = -v_A \frac{\partial T(x, t)_{A\xi}}{\partial x} + \frac{k}{\rho C_f} \frac{\partial}{\partial x} \left(\frac{\partial T(x, t)_{A\xi}}{\partial x} \right) - \frac{\Delta H k_{A o} e^{-\left(\frac{E}{RT_{A\xi}}\right)} \Psi(x, t)_{A\xi}}{\rho C_f}, x_L \leq x \leq x_A, t \geq 0 \quad (10)$$

$$\frac{\partial \Psi(x, t)_{A\xi}}{\partial t} = -v \frac{\partial \Psi(x, t)_{A\xi}}{\partial x} + D \frac{\partial^2 \Psi(x, t)_{A\xi}}{\partial x^2} - k_{A o} e^{-\left(\frac{E}{RT_{A\xi}}\right)} \Psi(x, t)_{A\xi}, x_L \leq x \leq x_A, t \geq 0 \quad (11)$$

$$\frac{\partial T(x, t)_{B\xi}}{\partial t} = -v_B \frac{\partial T(x, t)_{B\xi}}{\partial x} + \frac{k}{\rho C_f} \frac{\partial}{\partial x} \left(\frac{\partial T(x, t)_{B\xi}}{\partial x} \right) - \frac{\Delta H k_{B o} e^{-\left(\frac{E}{RT_{B\xi}}\right)} \Psi(x, t)_{B\xi}}{\rho C_f}, x_A \leq x \leq x_B, t \geq 0 \quad (12)$$

$$\frac{\partial \Psi(x, t)_{B\xi}}{\partial t} = -v \frac{\partial \Psi(x, t)_{B\xi}}{\partial x} + D \frac{\partial^2 \Psi(x, t)_{B\xi}}{\partial x^2} - k_{B o} e^{-\left(\frac{E}{RT_{B\xi}}\right)} \Psi(x, t)_{B\xi}, x_A \leq x \leq x_B, t \geq 0 \quad (13)$$

$$\frac{\partial T(x, t)_{C\xi}}{\partial t} = -v_C \frac{\partial T(x, t)_{C\xi}}{\partial x} + \frac{k}{\rho C_f} \frac{\partial}{\partial x} \left(\frac{\partial T(x, t)_{C\xi}}{\partial x} \right) - \frac{\Delta H k_{C o} e^{-\left(\frac{E}{RT_{C\xi}}\right)} \Psi(x, t)_{C\xi}}{\rho C_f}, x_B \leq x \leq x_C, t \geq 0 \quad (14)$$

$$\frac{\partial \Psi(x, t)_{C\xi}}{\partial t} = -v \frac{\partial \Psi(x, t)_{C\xi}}{\partial x} + D \frac{\partial^2 \Psi(x, t)_{C\xi}}{\partial x^2} - k_{C o} e^{-\left(\frac{E}{RT_{C\xi}}\right)} \Psi(x, t)_{C\xi}, x_B \leq x \leq x_C, t \geq 0 \quad (15)$$

$$\frac{\partial T(x, t)_{D\xi}}{\partial t} = -v_D \frac{\partial T(x, t)_{D\xi}}{\partial x} + \frac{k}{\rho C_f} \frac{\partial}{\partial x} \left(\frac{\partial T(x, t)_{D\xi}}{\partial x} \right) - \frac{\Delta H k_{D o} e^{-\left(\frac{E}{RT_{D\xi}}\right)} \Psi(x, t)_{D\xi}}{\rho C_f}, x_C \leq x \leq x_D, t \geq 0 \quad (16)$$

$$\frac{\partial \Psi(x, t)_{D\xi}}{\partial t} = -v \frac{\partial \Psi(x, t)_{D\xi}}{\partial x} + D \frac{\partial^2 \Psi(x, t)_{D\xi}}{\partial x^2} - k_{D o} e^{-\left(\frac{E}{RT_{D\xi}}\right)} \Psi(x, t)_{D\xi}, x_C \leq x \leq x_D, t \geq 0 \quad (17)$$

$$\frac{\partial T(x, t)_{E\xi}}{\partial t} = -v_E \frac{\partial T(x, t)_{E\xi}}{\partial x} + \frac{k}{\rho C_f} \frac{\partial}{\partial x} \left(\frac{\partial T(x, t)_{E\xi}}{\partial x} \right) - \frac{\Delta H k_{E o} e^{-\left(\frac{E}{RT_{E\xi}}\right)} \Psi(x, t)_{E\xi}}{\rho C_f}, x_D \leq x \leq x_{\mu}, t \geq 0 \quad (18)$$

$$\frac{\partial \Psi(x, t)_{E\xi}}{\partial t} = -v \frac{\partial \Psi(x, t)_{E\xi}}{\partial x} + D \frac{\partial^2 \Psi(x, t)_{E\xi}}{\partial x^2} - k_{Eo} e^{-\left(\frac{E}{RT_{E\xi}}\right)} \Psi(x, t)_{E\xi}, x_D \leq x \leq x_\mu, t \geq 0$$

Observe that each of equations (10)-(19) is valid in specified domains of definition in each compartment of the system. It should be noted that since equations (10)-(19) have PDEs with first order derivatives in time t and second order

derivatives in space, each will have one initial condition and two boundary conditions in each compartment of the system shown in Figure 1.

For $\gamma=\mathbf{A}$, equation (10) has initial and boundary conditions

$$T(x, 0)_{A\xi} = T(x)_{A\xi_0}$$

$$T(x = x_L, t)_{A\xi} = T(t)_{A\xi}$$

$$T(x = x_A, t)_{A\xi} = hT_w - hT(x = x_A, t)_{B\xi}$$

and equation (11) has initial and boundary conditions

$$\Psi(x, 0)_{A\xi} = \Psi(x)_{A\xi_0}$$

$$\Psi(x = x_L, t)_{A\xi} = \Psi(t)_{A\xi}$$

$$\Psi(x = x_A, t)_{A\xi} = k\Psi(x = x_A, t)_{B\xi}$$

For $\gamma=\mathbf{B,C}$ and \mathbf{D} , the initial and boundary conditions for (12), (14), and (16) are

$$T(x, 0)_{\gamma\xi} = T(x)_{\gamma\xi_0}$$

$$\frac{\partial T(x = x_{\gamma^*}, t)_{\gamma\xi}}{\partial x} = \frac{\left(\frac{k}{\rho C_f}\right)_{\gamma^*\xi}}{\left(\frac{k}{\rho C_f}\right)_{\gamma\xi}} \frac{\partial T(x = x_{\gamma^*}, t)_{\gamma^*\xi}}{\partial x}$$

$$T(x = x_\gamma, t)_{\gamma\xi} = hT_w - hT(x = x_\gamma, t)_{\gamma^*\xi}$$

and equations (13), (15) and (17) have initial and boundary conditions

$$\Psi(x, 0)_{\gamma\xi} = \Psi(x)_{\gamma\xi_0}$$

$$\frac{\partial \Psi(x = x_{\gamma^*}, t)_{\gamma\xi}}{\partial x} = \frac{D_{\gamma^*\xi}}{D_{\gamma\xi}} \frac{\partial \Psi(x = x_{\gamma^*}, t)_{\gamma^*\xi}}{\partial x}$$

$$\Psi(x = x_\gamma, t)_{\gamma\xi} = k\Psi(x = x_\gamma, t)_{\gamma^*\xi}$$

For $\gamma=\mathbf{E}$, equation (18) has initial and boundary conditions

$$T(x, 0)_{E\xi} = T(x)_{E\xi_0}$$

$$\frac{\partial T(x = x_D, t)_{E\xi}}{\partial x} = \frac{\left(\frac{k}{\rho C_f}\right)_{D\xi}}{\left(\frac{k}{\rho C_f}\right)_{E\xi}} \frac{\partial T(x = x_D, t)_{D\xi}}{\partial x}$$

$$T(x = x_\mu, t)_{E\xi} = hT_w - hT(x = x_\mu, t)_{E\xi}$$

and equations (13), (15) and (17) have initial and boundary conditions

$$\Psi(x, 0)_{E\xi} = \Psi(x)_{E\xi_0}$$

$$\frac{\partial \Psi(x = x_D, t)_{E\xi}}{\partial x} = \frac{D_{D\xi}}{D_{E\xi}} \frac{\partial \Psi(x = x_D, t)_{D\xi}}{\partial x}$$

$$\Psi(x = x_\mu, t)_{E\xi} = \Psi(x = x_\mu, t)_{E\xi_0}$$

where k in equations (10), (12), (14), (16) and (18) represents thermal conductivity, h and T_w in equations (22), (28) and (34) represent heat transfer coefficient and wall temperature respectively. Also γ^{-*} represents a compartment preceding γ^{th} compartment, γ^{+*} represents a compartment after γ^{th} compartment shown in Figure 1. This means that if $\gamma = B$, then γ^{-*} means $\gamma = A$ and γ^{+*} means $\gamma = C$ for $\gamma \in \{A, B, C, D, E\}$. It should be noted that Dirichlet boundary conditions (21), (22), (24), (25), (28), (31), (34), and (37) indicate assigned values at specified boundaries of the system shown in Figure 1. Also equations (27), (30), (33) and (36) show continuity of heat and mass flux from preceding γ^{-*} compartment to the next γ^{+*} compartment in a way showing relationship at the boundaries of Figure 1.

2.1 Well-posedness of the governing model (10) -(37)

The solution of the governing model PDEs together with their initial and boundary conditions (10) -(37) exist and are unique. Hence the system of PDEs consists of equations that are well-posed. Detailed analysis of well-posedness of the governing model PDEs (10)-(37) will not be considered here to avoid repetition. Readers may consult (Kreiss, & Lorenz, 1989; Strikwerda 1977) for extensive coverage of existence and uniqueness of their solutions.

2. Numerical Simulation

The numerical solution of the system of PDEs together with their auxiliary conditions (10) -(37) are obtained with the use of Method of Lines (MOL) technique. This technique involves discretisation of spatial derivatives of the governing model equations (10)-(37). In this study, finite difference approximations are used. Thus, let $i \in \square$ be an index representing

positions on grids in x such that $x = x_i$, then the first order derivative of equations (10)-(37) are

discretised using first order approximations to $\frac{\partial T}{\partial x}$ and $\frac{\partial \Psi}{\partial x}$ as

$$\frac{\partial T(x, t)}{\partial x} \approx \frac{T_i - T_{i-1}}{\Delta x} + O(\Delta x)$$

$$\frac{\partial \Psi(x, t)}{\partial x} \approx \frac{\Psi_i - \Psi_{i-1}}{\Delta x} + O(\Delta x)$$

and the second order derivative of the PDEs are discretised using second order approximations to $\frac{\partial^2 T}{\partial x^2}$

and $\frac{\partial^2 \Psi}{\partial x^2}$ as

$$\frac{\partial^2 T(x, t)}{\partial x^2} \approx \frac{T_{i+1} - 2T_i + T_{i-1}}{\Delta x^2} + O(\Delta x^2)$$

$$\frac{\partial^2 \Psi(x, t)}{\partial x^2} \approx \frac{\Psi_{i+1} - 2\Psi_i + \Psi_{i-1}}{\Delta x^2} + O(\Delta x^2)$$

where $O(\Delta x)$ and $O(\Delta x^2)$ are truncation errors of approximations from Taylor series.

$i=1$ and last boundary (right-end) with $i=M$ in x. Substitution of (38) -(41) into governing model equations (10) -(19) gives

Let total number of grids in x be M such that each compartment has first boundary (left end) with

$$\frac{dT(t)_{(\gamma\xi) i}}{dt} = -v_\gamma \frac{T(t)_{(\gamma\xi) i} - T(t)_{(\gamma\xi) i-1}}{\Delta x}$$

$$+ \frac{k}{\rho C_f} \left[\frac{T(t)_{(\gamma\xi) i+1} - 2T(t)_{(\gamma\xi) i} + T(t)_{(\gamma\xi) i-1}}{\Delta x^2} \right]$$

$$- \frac{\Delta H k_{\gamma o} e^{-\left(\frac{E}{RT_{\gamma\xi}}\right)} \Psi(t)_{(\gamma\xi) i}}{\rho C_f}, 1 \leq i \leq M_{(\gamma)}, t \geq 0;$$

$$\frac{d\Psi(t)_{(\gamma\xi) i}}{dt} = -\nu \frac{\Psi(t)_{(\gamma\xi) i} - \Psi(t)_{(\gamma\xi) i-1}}{\Delta x} + D \left[\frac{\Psi(t)_{(\gamma\xi) i+1} - 2\Psi(t)_{(\gamma\xi) i} + \Psi(t)_{(\gamma\xi) i-1}}{\Delta x^2} \right] - k_{\gamma o} e^{-\left(\frac{E}{RT_{\gamma\xi}}\right)} \Psi(t)_{(\gamma\xi) i}, 1 \leq i \leq M_{(\gamma)}, t \geq 0;$$

where M_{γ} represent number of grid points in x for each γ^{th} compartment of Figure 1.

Initial and boundary conditions (20), (21) and (22) for $\gamma = A$ are semi-discretised as

$$\begin{aligned} T(t=0)_{(A\xi) i} &= T(x(i))_{A\xi 0} \\ T(t)_{(A\xi) 1} &= T(t)_{A\xi} \\ T(t)_{(A\xi) M(A)} &= hT_w - hT(t)_{(\beta\xi)M(A)} \end{aligned}$$

and initial and boundary conditions (23), (24) and (25) are semi-discretised as

$$\begin{aligned} \Psi(t=0)_{(A\xi) i} &= \Psi(x(i))_{A\xi 0} \\ \Psi(t)_{(A\xi) 1} &= \Psi(t)_{A\xi} \\ \Psi(t)_{(A\xi) M(A)} &= k\Psi(t)_{(\beta\xi)M(A)} \end{aligned}$$

Also initial and boundary conditions (26), (27) and (28) of γ^{th} compartment for $\gamma \in \{B, C, D\}$ are semi-discretised as

$$\begin{aligned} T(t=0)_{(\gamma\xi) i} &= T(x(i))_{\gamma\xi 0} \\ \frac{T(t)_{(\gamma\xi) M_{(\gamma^{*-})}} - T(t)_{(\gamma\xi) M_{(\gamma^{*-})}-1}}{\Delta x} &= \frac{\left(\frac{k}{\rho C_f}\right)_{(\gamma^{*-})} T(t)_{[(\gamma^{*-})\xi] M_{(\gamma^{*-})}} - T(t)_{[(\gamma^{*-})\xi] M_{(\gamma^{*-})}-1}}{\Delta x} \\ &\quad \frac{\left(\frac{k}{\rho C_f}\right)_{(\gamma)}}{\Delta x} \\ T(t)_{(\gamma\xi) M_{(\gamma)}} &= hT_w - hT(t)_{(\gamma^{+*})\xi M_{(\gamma)}} \end{aligned}$$

and initial and boundary conditions (29), (30) and (31) are semi-discretised as

$$\Psi(t = 0)_{(\gamma\xi) i} = \Psi(x(i))_{\gamma\xi 0}$$

$$\frac{\Psi(t)_{(\gamma\xi) M_{(\gamma^*)}} - \Psi(t)_{(\gamma\xi) M_{(\gamma^*)-1}}}{\Delta x} = \frac{D_{(\gamma^*)}}{D_{(\gamma)}} \frac{\Psi(t)_{[(\gamma^*)\xi] M_{(\gamma^*)}} - \Psi(t)_{[(\gamma^*)\xi] M_{(\gamma^*)-1}}}{\Delta x}$$

$$\Psi(t)_{(\gamma\xi) M_{(\gamma)}} = k\Psi(t)_{(\gamma^*)\xi M_{(\gamma)}}$$

For initial and boundary conditions (32), (33) and (34) for $\gamma = E$, the following semi-discretised system of equations are obtained

$$T(t = 0)_{(E\xi) i} = T(x(i))_{E\xi 0}$$

$$\frac{T(t)_{(E\xi) M_{(D)}} - T(t)_{(E\xi) M_{(D)}-1}}{\Delta x} = \frac{\left(\frac{k}{\rho C_f}\right)_{(D)}}{\left(\frac{k}{\rho C_f}\right)_{(E)}} \frac{T(t)_{(D\xi) M_{(D)}} - T(t)_{(D)\xi M_{(D)}-1}}{\Delta x}$$

$$T(t)_{(\gamma\xi) M_{(\gamma)}} = hT_w - hT(t)_{(\gamma^*)\xi M_{(\gamma)}}$$

and initial and boundary conditions (35), (36) and (37) for $\gamma = E$ gives semi-discretised equations as

$$\Psi(t = 0)_{(E\xi) i} = \Psi(x(i))_{E\xi 0}$$

$$\frac{\Psi(t)_{(E\xi) M_{(D)}} - \Psi(t)_{(E\xi) M_{(D)}-1}}{\Delta x} = \frac{D_{(D)}}{D_{(E)}} \frac{\Psi(t)_{(D\xi) M_{(D)}} - \Psi(t)_{(D)\xi M_{(D)}-1}}{\Delta x}$$

$$\Psi(t)_{(E\xi) M_{(E)}} = \Psi(t)_{E\xi_0 M_{(E)}}$$

The semi-discretised system of equations (42) and (43) will be solved in each compartment together with their auxiliary conditions (44)-(61) for the non isothermal multiple-compartment system shown in Figure 1.

3. Results and Discussion

The schematic representation of species transport through non isothermal multiple-compartment

system is shown in Figure 1. The total length of the entire multiple-compartment system is 600m so that each compartment is 120m long. The grid points $M_{(\gamma)}$, $\gamma \in \{A, B, C, D, E\}$ used for the numerical simulation of the governing model equations in this study are taken to be 21 in each compartment of the chemical reactor system. Thus, semi-discrete systems of ODEs which

resulted from the coupled system of (10) – (37) are solved simultaneously for parameters of endothermic reaction from the pyrolysis of propane selected from literature (Bornakke & Sonntag, 1996; Hill, 1977; Knacke *et al.*, 1991; Nighswander, 1989; Perry & Chilton, 1973; Rastogi *et al.*, 1988) with some values converted to S.I units. Fluid specific heat $C_f = 0.8303$ cal/g.K, thermal conductivity $k = 1.787 \times 10^{-4} (cal.cm) / s.cm^2.k$, heat of reaction $\Delta H = 21960$ cal/gmol, specific rate constant $k_{\gamma_o} = 3.98 \times 10^{12}$ cal / gmol , activation energy $E = 59100$ cal/gmol.K, mass diffusivity $D_\gamma = 9 \times 10^3$ cm^2 / s , linear fluid velocity $v = 0.01$ cm/s, initial temperature $T_{\gamma_o} = 866.48K$, initial concentration of

species $T_{\gamma_o} = 866.48K$
 $\Psi(x)_{\gamma_o} = 40 gmol / cm^3$, wall temperature $T_w = 1074.82K$, heat transfer coefficient $h = 0.01$ cal / (s.cm².k), fluid density $\rho = 6.14 \times 10^{-4}$ g / cm³, gas constant $R = 1.987$ cal / gmol.k, and from the entry point, a constant boundary value of $\Psi(x)_{\gamma_o} = 40 gmol / cm^3$ is used. Results from the simulation of the semi-discrete systems obtained from (10)-(37) with the aid of Matlab ode15s are shown in Figures 2,3,4,5,6 and 7 for temperature and concentration profiles of species being transported through interconnected non isothermal (q=5) multiple-compartment system at times t = 10 seconds, 120 seconds and 12,000 seconds (3 hours 20 minutes).

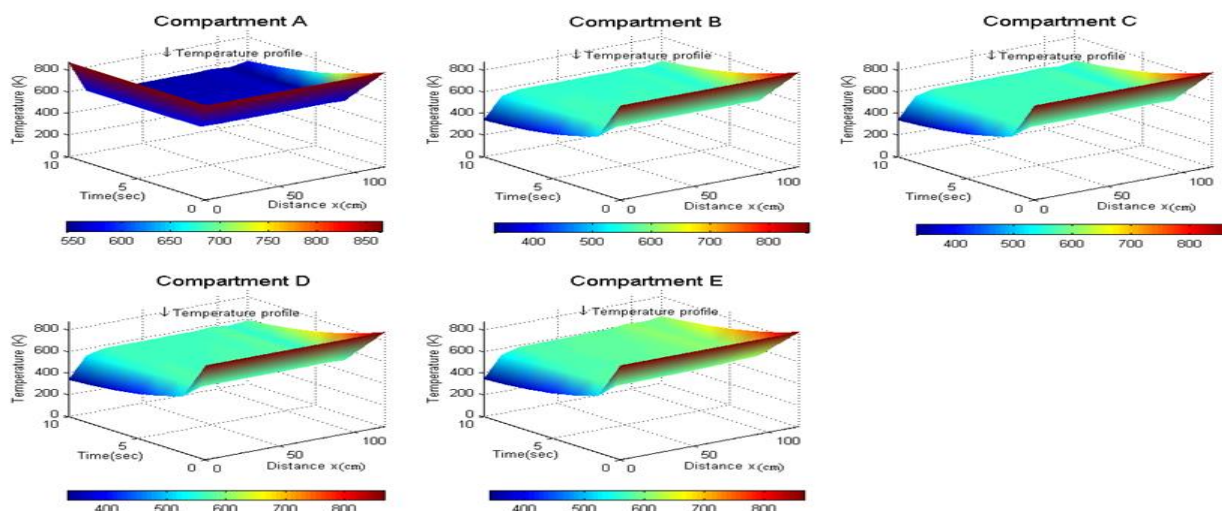


Figure 2: Temperature profile of species in multiple-compartment system at t = 10 seconds

While Figure 2 shows axial variation of small temperature changes at t = 10 seconds, Figure 3 indicate significant decrease in temperature along x-axis. This means that as the reactant chemical species spatially moves through the reactor

system, heat is absorbed due to significant conversion of the reactant in the reactor by the endothermic reaction causing a temperature decrease.

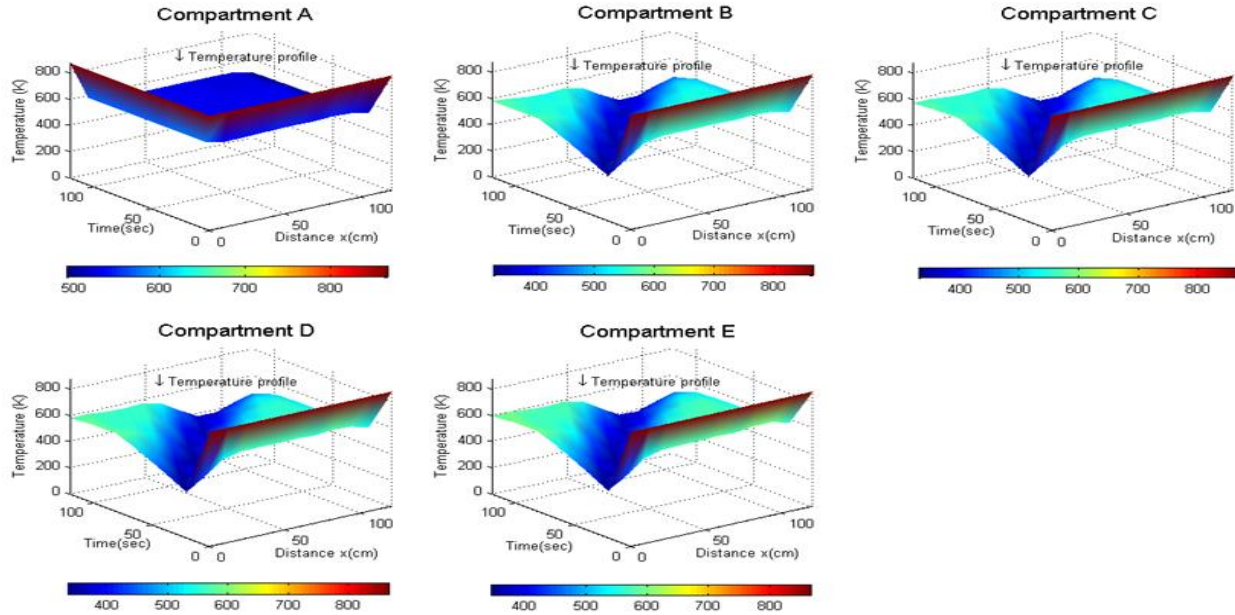


Figure 3: Temperature profile of species in multiple-compartment system at $t = 120$ seconds

However, temperature begins rise due to the effect of wall temperature until it approaches steady state as shown in Figure 4 where

noticeable changes do not appear after significant conversion of the reactant has been accomplished.

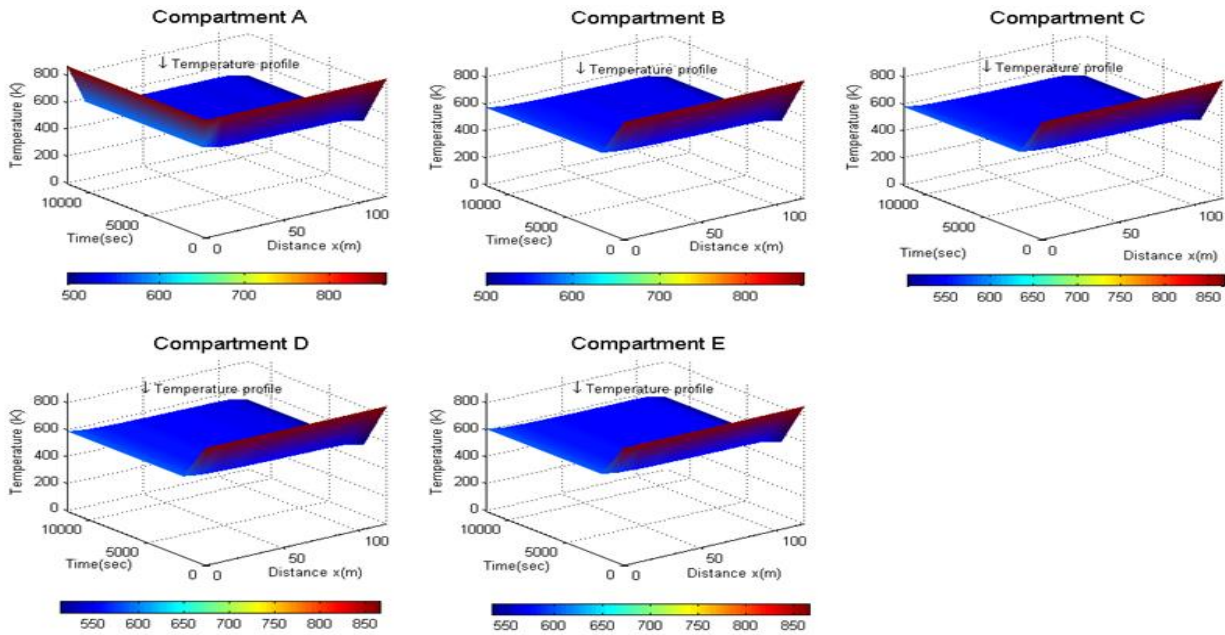


Figure 4: Temperature profile of species in multiple-compartment system at $t = 12,000$ seconds.

It can be seen that the temperature T_r falls from entering value of 866.48 K as the chemical

species moves through the length of the reactor and attains a steady value of 499.09 K at exit.

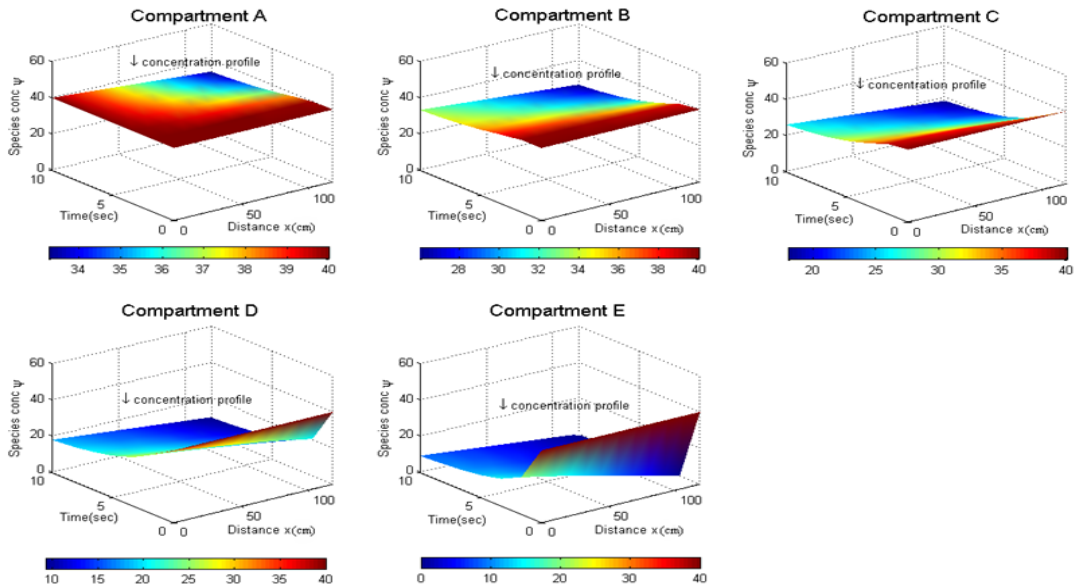


Figure 5: Concentration profile of species in multiple-compartment system at $t = 10$ seconds.

The concentration profile of species with initial concentration $40 \text{ gmol} / \text{cm}^3$, being transported through the non isothermal system is shown in Figure 5 at $t = 10$ seconds.

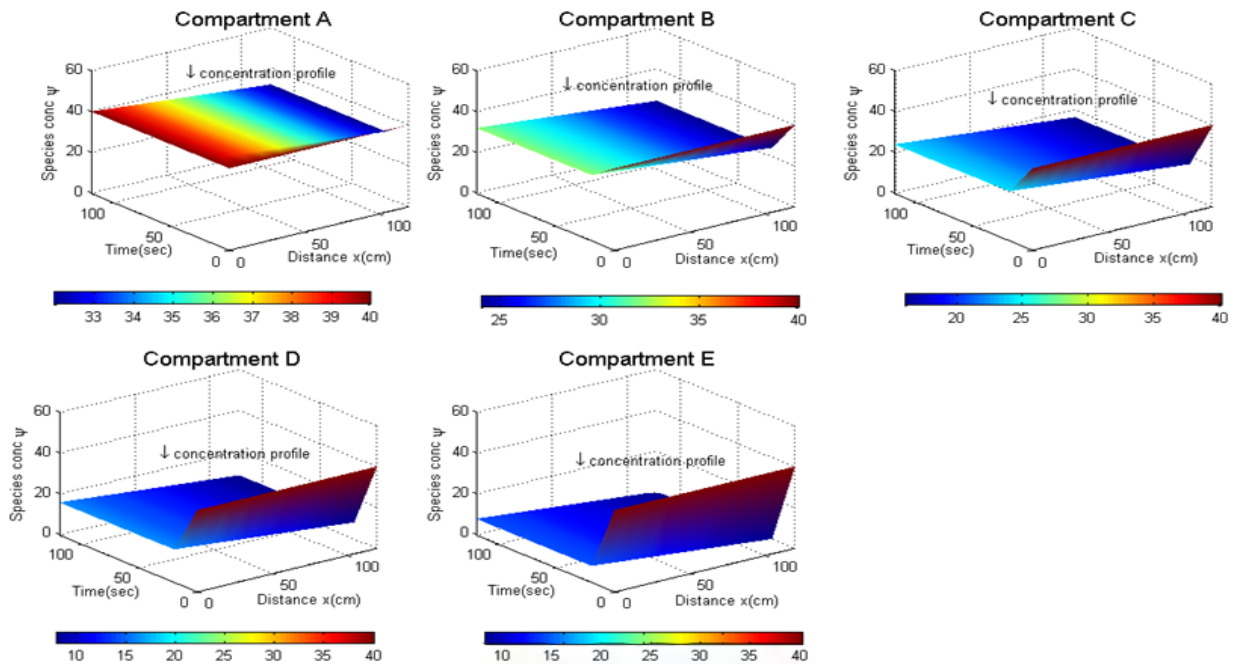


Figure 6: Concentration profile of species in multiple-compartment system at $t = 120$ seconds.

Figure 6 shows the concentration profile of species with diffusivity $9 \times 10^3 \text{ cm}^2 / \text{s}$ at time $t = 120$ seconds and finally Figure 23(7) shows concentration profile at $t=12,000$ seconds (3hours 20minutes).

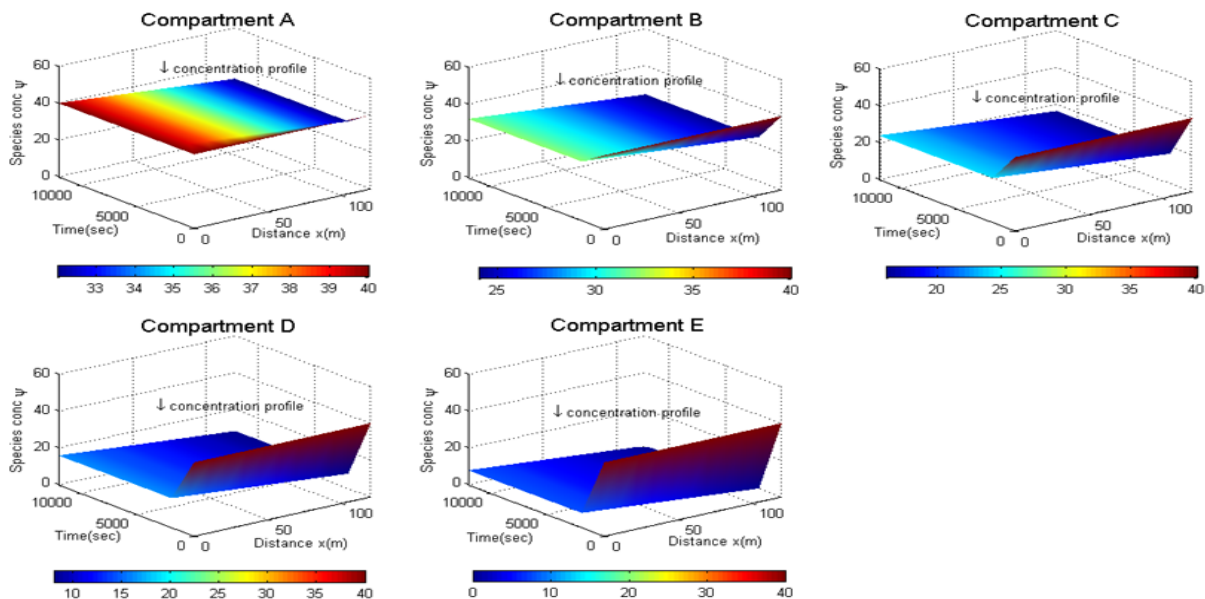


Figure 7: Concentration profile of species in multiple-compartment system at $t = 12,000$ seconds.

It can be seen from Figures 5, 6 and 7 that as time t progresses, there is a reduction in concentration profile due to consumption of the chemical species in the interconnected non isothermal multiple-compartment system along x -axis. It can also be observed from results indicated in Figure 7 that the values of concentration at the end of one boundary and the beginning of another boundary of each interconnected compartment of the system are 32.00 g/cm^3 , 24.00 g/cm^3 , 16.00 g/cm^3 and 8.00 g/cm^3 . respectively at $t=12,000$ seconds (3 hours 20 minutes).

4. Conclusion

In this paper, a mathematical model for transport of chemical species through non isothermal interconnected multiple-compartment system is developed. The focus is to investigate temperature and concentration profiles in nonisothermal system that consists of adjacent

compartments which are connected at their boundaries. Transport of chemical species involving endothermic reaction is considered with requirement that thermal energy has to be supplied to the interconnected system at an elevated temperature. This necessitates that transmission of heat would be of a particular importance in determining temperature profile. Particularly, this study used process parameters for pyrolysis of propane in the production of ethylene. Results obtained show decrease in temperature at some time t along the reactor length. This indicates that as reactant chemical species moves spatially through the system, heat is absorbed due to significant conversion in chemical reaction of the species being transported causing a decrease in temperature. However, after some time t , temperature begins rise due to constant wall temperature until a steady state is attained when significant conversion of reactant has been accomplished. Further results from the

mass balance equations whose reaction terms are coupled to energy balance equations also indicate a reduction in concentration profile due to consumption of the chemical species as the spatial distance it covers increases in the multiple-compartment system. Hence, the developed model is recommended for use in interconnected systems where reaction rate constant of kinetic model depends on temperatures changes for a chemical species undergoing first order reaction kinetic.

References

- Adedire, O., and Ndam, J. N. (2020a). Mathematical modelling of concentration profiles for species transport through the single and the interconnected multiple-compartment systems. *Journal of the Nigerian Society of Physical Sciences*, 2, 61-68.
- Adedire, O., and Ndam, J. N. (2020b). Theoretical comparison of linear and nonlinear boundary sinks for species transport in isothermal multiple-compartment reactors. *Open Journal of Mathematical Sciences*, 4, 280-289, doi:10.30538/oms2020.0119.
- Adedire, O., Ndam, J. N. (2019). Mathematical modeling of chlorine decay through water and intermediate pseudomonas aeruginosa in multiple-compartment isothermal reactor. *Journal of Advanced Mathematical Models and Applications*, 4(2), 167-178.
- Audenaert, W.T.M., Callewaert, M., Nopens, I., Cromphout, J., Vanhoucke, R., Dumoulin, A., A., Dejans, P., & Van Hulle, S.W.H. (2010). Full-scale modelling of an ozone reactor for drinking water treatment. *Chemical Engineering Journal*, 157, 551-557.
- Ball, D. K. (1998). Kinetics of Consecutive Reactions: First Reaction, First-Order; Second Reaction, Zero th-Order. *Journal Chemical Education*, 75, 917-918
- Borisov, M., Dimitrova, N., & Beschkov, V. (2012). Stability analysis of a bioreactor model for biodegradation of xenobiotics. *Journal of Computer and Mathematics with Applications*, 64, 361-373.
- Bornakke, C., & Sonntag, R.E. (1996). *Tables of thermodynamics and transport properties*. New York: John Wiley & Sons.
- Chick, H. (1908). An investigation of the laws of disinfection. *Journal of Hygiene*, 8, 92-158.
- Connors, K. (1990). *Chemical kinetics: The study of reaction rates in solution*. New York: VCH Publishers, Inc.
- Crank, J. (1979). *The mathematics of diffusion*. Oxford university press.
- Crapulli, F., Domenico, S., Haas, N.C., Notarnicola, M., & Liberti, L. (2010). Modelling virus transport and inactivation in a fluoropolymer tube UV photoreactor using computational fluid dynamics. *Journal of Chemical Engineering*, 161, 9-18.
- Hill, C.J. (1977). *An introduction to chemical engineering kinetics and reactor design*. New York: John Wiley & Sons.
- Kiss, V., & Osz, K. (2017). Double Exponential Evaluation under Non-Pseudo-First-Order Conditions: A Mixed Second-Order Process Followed by a First-Order Reaction.

- International Journal of Chemical Kinetics*, 49, 602-610. doi 10.1002/kin.21100
- Knacke, O., Kubaschewski, O., & Hesselmann, K. (1991). *Thermochemical properties of inorganic substances* (2nd ed.). Berlin: Springer-verlag.
- Kreiss, H., & Lorenz, J. (1989). *Initial-boundary value problems and the Navier-Stokes Equation* San Diego: Academic Press, Inc.
- Manion, J. A., Mcgovern, W. S. (2016). The importance of relative reaction rates in the optimisation of detailed kinetic models, *International Journal of Chemical Kinetics*, 48 358-366. <https://doi.org/10.1002/Kin.20996>.
- Nelson, M.I., & Balakrishnan, E. (2008). Auto ignition of hydrocarbons in a batch reactor: Analysis of a reduced model. *Journal of Applied Mathematics Letters*, 21, 866-871.
- Nighswander, J.A., Huntroids, R.S., Mehrotra, A.K., & Behie, L.A. (1989). Quench time modelling in propane ultrapyrolysis. *The Canadian Journal of Chemical Engineering*, 67, 608-614.
- Orava, V., Soucek, O., & Cendula, P. (2015). Multi-phase modelling of non-isothermal reactive flow in fluidized bed reactors. *Journal of Computational and Applied Mathematics*, 289, 282-295.
- Perry, R. H., & Chilton, C.H. (1973). *Chemical engineers' handbook* (5th ed.). New York: McGraw -Hill.
- Rastogi, A., Svrcek, W.Y., & Behie, L.E. (1988). The importance of temperature rise in pyrolysis kinetic studies. *The Canadian Journal of Chemical Engineering*, 66, 303-306.
- Sharma, A.K., Birgersson, E., & Vynnycky, M. (2015). Towards computationally-efficient modeling of transport phenomena in three-dimensional monolithic channels. *Journal of Applied Mathematics and Computation*, 254, 392-407.
- Strikwerda, J. (1977). Initial boundary value problems for incomplete parabolic systems. *Journal of Communications on Pure and Applied Mathematics*, 30, 797-822.
- Thompson, P.A. (1972). *Compressible-fluid dynamics*. New York: McGraw-Hill, Inc.
- Tyrrell, H.J.V. (1964). The origin and present status of Fick's diffusion law. *Journal of Chemical Education*, 41(7), 397-400.
- Watson, H.E. (1908). A note on the variation of rate of disinfection with the change in concentration of the disinfectant. *Journal of Hygiene*, 8, 536-542.